JOURNAL OF VIROLOGY, Apr. 1993, p. 1830–1839
0022-538X/93/041830-10$02.00/0
Copyright © 1993, American Society for Microbiology
Vol. 67, No. 4

Bovine Leukemia Virus RNA Sequences Involved in Dimerization and Specific *gag* Protein Binding: Close Relation to the Packaging Sites of Avian, Murine, and Human Retroviruses

IYOKO KATOH,[1]* TERUO YASUNAGA,[2]† AND YOSHIYUKI YOSHINAKA[1]

Microbiological Research Institute, Otsuka Pharmaceutical Co., Ltd., 463-10 Kagasuno, Kawauchi, Tokushima 771-01,[1] and Computation Center, The Institute of Chemical and Physical Research, 2-1 Hirosawa, Saitama 351-01,[2] Japan

Received 1 September 1992/Accepted 15 December 1992

In vitro detection of a specific complex of the bovine leukemia virus (BLV) MA(p15) protein and the 5′-terminal RNA dimer led to the hypothesis that the NH_2-terminal domain of retrovirus *gag* protein precursor is involved in the selective viral RNA packaging mechanism. Here we describe mapping of the BLV RNA for dimer-forming and MA(p15)-binding abilities by a simple cDNA probing method followed by mutation analyses with the reactive U5-5′ *gag* RNA. The RNA dimerization is mediated by the region harboring U5, the primer binding site (PBS), and the 30 bases immediately downstream of PBS. This conclusion is supported by computer-assisted RNA secondary-structure analysis which predicted a multibranched stem-loop folding throughout the dimer region determined. Another region from PBS to the 5′-terminal 60 residues of the *gag* gene, partially overlapping the dimer region, likely provides essential elements for the MA(p15) binding reaction, although the presence of either the 3′ or 5′ neighboring sequences increases the complex-forming efficiency significantly, and each of the substructures predicted within the core region has, if any, only very weak affinity to MA(p15). These in vitro characterizations of the BLV RNA may reflect general features of the specific protein-RNA interaction in the packaging events of various retroviruses. 5′-terminal folded structures of retroviral RNA molecules and their biological activities are discussed.

Although the molecular mechanism of retrovirus replication has been characterized to a great extent, several critical processes remain to be explained. Among them is the stage of virus particle formation, the stage at which assembly of the *gag* precursor polyprotein and specific association of a domain of the precursor with viral RNA are thought to be primary biochemical events leading to productive virus morphogenesis.

Two schools of evidence have been presented in the study of the virus protein-RNA interaction. Results of in vitro mutagenesis experiments emphasized that the COOH-terminal nucleocapsid (NC) domain of the *gag* precursor and its zinc finger-like motifs are required for viral RNA packaging (3, 9, 10, 15, 29–31). Direct RNA binding experiments with purified viral proteins suggested that the NH_2-terminal domain of the matrix-associated (MA) protein or its adjacent polypeptide plays the key role (17, 21, 39, 40). The NC protein was shown to be a nonspecific RNA-binding protein (16, 17, 20) that forms the viral nucleocapsid complex.

On the other hand, location of the packaging signal in the genome RNA has been assessed by deletion and recombination analyses, and no significant difference among the relative positions determined for retroviruses of various species has been found (3, 18, 23, 28, 33, 41, 43, 45). Recent results of detailed examinations of murine leukemia virus (MuLV) and Rous sarcoma virus, however, indicate that packaging sequences should be in a more extended region than was originally determined (1, 5–7, 24). Another intriguing feature of retroviral genome encapsidation is that the viral RNA is incorporated into the particles as a dimer of the identical molecule. It has long been postulated that the dimer structure is closely related to the packaging events. Although hypothetical dimer models were deduced from possible base pairings within the 5′-terminal RNA sequences, their probabilities have not been experimentally validated (8, 13). Recently, the presence of a folded structure of a stem-loop with multiple branches has been reported for the *cis* packaging element of human immunodeficiency virus type 1 (HIV-1) on the basis of computer analysis in combination with enzyme and chemical probing experiments (12). As yet, however, no direct in vitro evidence points to the folded structure as the signal recognized by the HIV *gag* precursor protein (26).

Here we show that minimum elements required for bovine leukemia virus (BLV) RNA dimerization and complex formation with MA(p15) are located in a region corresponding to the packaging site determined for various retroviruses. Our electrophoretic analysis of the protein-RNA interaction may account for one of the critical steps of retrovirus packaging of dimeric viral RNA.

MATERIALS AND METHODS

Purification of MA(p15). BLV was prepared from culture fluid of Bat2Cl1 cells (36) as described previously (17). MA(p15) was purified from the BLV preparations by acetone treatment followed by Sephacryl S-200 column chromatography and reverse-phase high-performance liquid chromatography (RP-HPLC) as described previously (17). The purified protein fraction was lyophilized, solubilized in H_2O with 0.025% Nonidet P-40, and quantitated by the Lowry method (25). The MA(p15) solution was adjusted to 50 μM and stored at 4°C.

Synthesis of RNA fragments. Viral RNA fragments and

* Corresponding author.
† Present address: Genome Information Research Center, Osaka University, 3-1 Yamadaoka, Suita City, Osaka 565, Japan.

their mutants were synthesized by the SP6 RNA polymerase reaction as described previously (17). ^{32}P-labeled U5-5′ *gag* and mutant RNAs were produced in reaction buffer (40 mM Tris-HCl [pH 7.5], 6 mM $MgCl_2$, 2 mM spermidine, 10 mM dithiothreitol, 1 U of human placenta RNase inhibitor (Takara) per μl) containing 0.5 mM each GTP, UTP, and ATP, 0.05 mM CTP, 0.025 mmol [α-^{32}P]CTP, 2 μg of linearized template DNA, and 20 U of SP6 RNA polymerase (Takara) in a total volume of 20 μl. Incubation was for 1 h at 37°C. Unlabeled U5-5′ *gag* was synthesized by incubating for 16 h at 37°C the following reaction mixture (50 μl): the same buffer containing 0.5 mM all four ribonucleoside triphosphates, 1 μg of pAM5G cleaved by *Sal*I (pAM5G/*Sal*I; *Sal*I from Boehringer Mannheim) per μl, and 30 U of the enzyme. After the polymerase reaction, the template was removed by DNase I (8 U) digestion for 10 min. Products were deproteinized by two extractions with phenol-chloroform-isoamyl alcohol (25:24:1) followed by one extraction with chloroform-isoamyl alcohol (24:1) and then precipitated with ethanol. Dried RNA was dissolved in H_2O and quantitated. Aliquots were stored at −70°C. For the MA(p15) binding assay, RNA solution was made on ice in 2× binding buffer containing 20 mM *N*-2-hydroxyethylpiperazine-*N*′-2-ethanesulfonic acid (HEPES; pH 7.9), 12 mM $MgCl_2$, 20 mM NaCl, 2 mM dithiothreitol, and 1 U of RNase inhibitor per μl.

cDNA probing. DNAs consisting of 18 or 30 bases complementary to the U5-5′ *gag* RNA sequences were synthesized by a DNA synthesizer (Applied Biosystems model 381A) and purified by RP-HPLC through a C_{18} column (Waters) with an acetonitrile gradient from 5 to 20% in 0.1 M triethylamine acetate (pH 7.0). In one set of experiments, synthetic cDNAs were 5′ end labeled with [γ-^{32}P]ATP (New England Nuclear) and T4 polynucleotide kinase (New England BioLabs), phenol extracted, and ethanol precipitated. Each labeled cDNA was added to the SP6 RNA polymerase reaction mixture (20 μl) containing pAM5G/*Sal*I (2 μg) and four unlabeled ribonucleoside triphosphates prior to incubation. In another set of cDNA probing assays, unlabeled synthetic cDNA was added to the RNA polymerase reaction to produce U5-5′ *gag* labeled with [α-^{32}P]CTP. Unlabeled ATP, GTP, and UTP were used at 0.5 mM each; CTP was adjusted to make a final concentration of 0.075 mM. Incubation was for 1 h at 37°C. DNase treatment was eliminated.

Construction of plasmids for the expression of mutant RNA segments. The wild-type plasmid previously referred to as pAMG has been renamed pAM5G for easier identification in comparison with various DNAs used in this work. Deletion and fusion mutants were newly constructed from parental plasmids pAM5G and pAMGPE (17). Their identities and construction methods are described below. Nucleotide positions were numbered in relation to the transcription start site, +1. DNA fragments generated by restriction enzyme digestions are always indicated below as A-B, representing the sequences from the 5′ end (A site) to the 3′ end (B site) in the orientation of the BLV coding sequences (38). In the case of noncohesive ligation, ends were blunted with T4 DNA polymerase prior to the ligation reaction unless specified otherwise. Plasmids obtained from transformants of *Escherichia coli* HB101 were screened by restriction enzyme mapping.

Construction of deletion mutants. (i) pAM5GdP. Plasmid pAM5G was cleaved into two fragments by digestion with *Bcl*I (at position +340) and *Xmn*I (at a unique site in the vector, pAM18 [Pharmacia]). One fragment, *Xmn*I-*Bcl*I (+340), was digested with *Bst*NI (+301) to remove the primer binding site (PBS) and ligated to the other fragment, *Bcl*I (+341)-*Xmn*I.

(ii) pAM5Gdα. The BLV U5-5′ *gag* sequences, +147 to +940, were excised from pAM5G by digestion with *Eco*RI and *Sph*I (at the unique cleavage sites derived from the multiple cloning site of the vector) and further digested with *Ava*II (+369) to remove the 5′-terminal sequences. The deleted fragment, *Ava*II (+370)-*Sph*I, was linked to the *Sal*I (in the multiple cloning site)-*Bcl*I (+340) fragment which contained the vector and the BLV sequences from +147 to +340.

(iii) pAM5GdPdα. pAM5GdPdα was constructed by the cohesive ligations of four DNA fragments, *Ava*II (+370)-*Sph*I, *Sph*I-*Xmn*I, *Xmn*I-*Bst*NI (+321), and a *Bst*NI-*Ava*II adaptor made by annealing two strands of synthetic oligonucleotides, 5′AGGAGA3′ and 3′CCTCTCTG5′.

(iv) pAM5Gdβ. pAM5G was incubated with *Ava*II to make a partial digestion. Linear forms were isolated, further cleaved by *Bss*HII (+487) to remove *Ava*II (+373)-*Bss*HII (+487), and recircularized.

(v) pAM5Gdαdβ. *Bcl*I (+345)-*Bss*HII (+487) sequences were removed by digestion of pAM5G with the two enzymes and recircularized.

(vi) pAM5GdPdαdβ. The *Xmn*I-*Bst*NI (+301) fragment was linked to the *Bss*HII (+488)-*Xmn*I fragment.

(vii) pAMLG. The *Bst*NI (+302)-*Sal*I (+936) fragment was isolated from pAM5G and inserted into the pAM18 vector at the *Sma*I cloning site.

(viii) pAMgag. The *Sac*I (+147)-*Dra*I (+535) region was deleted from pAM5G by digestion of the two enzymes.

Construction of recombinant mutants. *Hin*dIII (in the multiple cloning site)-*Bam*HI (+5015) sequences encoding the 3′ end of *gag* to the 5′ end of *env* were removed from pAMGPE to obtain fragment *Bam*HI (+5016)-*Hin*dIII (AME), which corresponds to the linear form of pAME (17). Recombinants between U5-5′ *gag* and the *env* gene were generated by inserting segments from U5-5′ *gag* between the *Hin*dIII and *Bam*HI ends of the AME fragment.

(i) pAM5LE and pAM(5L)E. The *Sac*I (+147)-*Bss*HII (+488) fragment was isolated from pAM5G and linked to the AME fragment. The resulting plasmids with sense and antisense insertions were called pAM5LE and pAM(5L)E, respectively.

(ii) pAMLE. The *Hae*II (+286)-*Bss*HII (+487) fragment was ligated to AME.

(iii) pAM5E. Similarly, the *Sac*I (+147)-*Hae*II (+290) sequences were inserted 5′ to the *env* region.

(iv) pAMα+E. Synthetic double-stranded DNA from positions +322 to +386 with 5′ *Hin*dIII and 3′ *Bam*HI cohesive ends was linked to AME.

(v) pAMα$^+$βE. The *Bam*HI(+5016)-*Apa*I (+5206) region of pAMα$^+$E was replaced by synthetic DNA from positions +410 to +471 with 5′ *Bam*HI and 3′ *Apa*I sticky ends.

(vi) pAMβE. pAMα$^+$βE was cleaved by *Hin*dIII and *Bam*HI to remove the α sequences and was then recircularized.

Plasmids containing the *gag* sequences were cleaved by *Sal*I, and those with the *env* sequences were cleaved by *Ava*II; the plasmids were then phenol extracted and ethanol precipitated as described above to serve as the templates for the RNA synthesis reaction.

Gel mobility shift assay. The RNA gel mobility shift assay was performed by modification of the methods described for the HIV Rev RNA-binding protein (14, 27) and those for various transcription factors that bind to their target DNA sequences (22). Briefly, RNA solution in 2× binding buffer

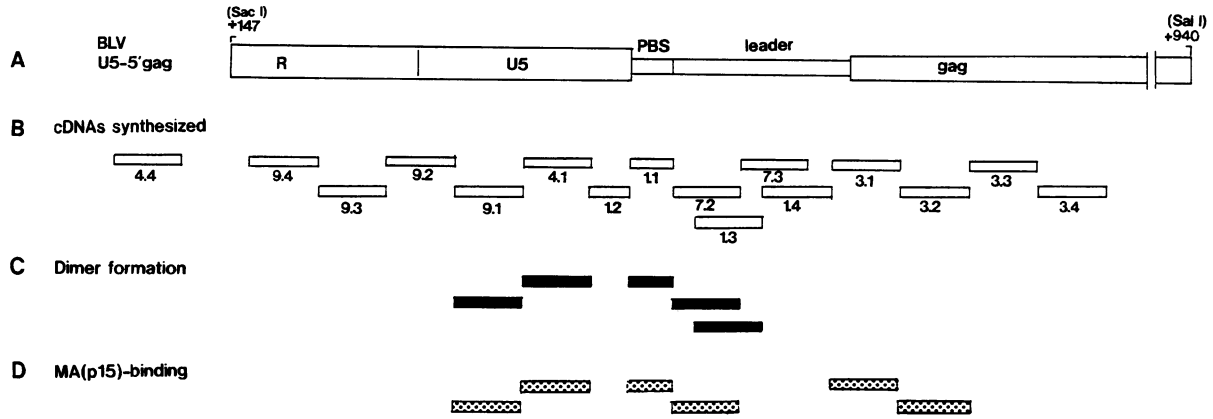

FIG. 1. Summary of cDNA probing assays. (A) Structure of the BLV U5-5′ *gag* RNA fragment. RNA encompassing the *Sac*I site at +147 to the *Sal*I site at +936 was in vitro synthesized. R, U5, PBS, leader, and *gag* regions are mapped. The 5′ splice donor site in the genome RNA is 47 bases upstream from the 5′ end of the U5-5′ *gag* segment. (B) cDNA probes. DNAs synthesized for probing assays are indicated by bars placed in their target sequences. cDNA 4.4 was complementary to +95 to +124, which were not contained in the RNA fragment. (C) Inhibition of RNA dimer formation. cDNAs that interfered with the RNA dimer formation in at least one of the two sets of probing assays are shown by filled bars. Probes 9.1, 4.1, 1.1, 7.2, and 1.3 had sequences complementary to +245 to +274, +275 to +304, +322 to +339, +340 to +369, and +350 to +379, respectively. (D) Alteration of the RNA mobility shift. cDNAs 1.1, 7.2, 3.1, and 3.2, which influenced complex formation with MA(p15), are indicated by dotted bars. Probes 3.1 and 3.2 were complementary to +410 to +439 and +440 to +469, respectively.

was mixed with MA(p15) protein solution at a ratio of 1:1 on ice and incubated for 10 min at 20°C. One volume of the loading buffer (30% glycerol, 0.02% xylene cyanol, 0.02% bromophenol blue) was added per 5 volumes of the reaction mixture, from which 3 μl was loaded per slot. Samples were run for 3 h at 120 V at 4°C. The electrophoresis gel was made of 2.5% polyacrylamide and 0.5% agarose in TBE buffer (90 mM Tris-borate, 2 mM EDTA [pH 8.0]).

Assay results were not affected either by NaCl concentration in the binding reaction within a range from 10 to 50 mM or by pH between 7.5 and 8.0. The presence of 100 mM NaCl reduced the band shift efficiency of U5-5′ *gag* by 30% without relaxing the binding specificity of MA(p15).

Prediction of the BLV RNA secondary structure. Minimum-energy secondary structures were constructed by operating a SUN computer with programs FOLDRNA and SQUIGGLES supplied by the University of Wisconsin Genetics Computer Group. BLV sequence data were from reference 38.

RESULTS

cDNA probing assays. To determine the functional map of the U5-5′ *gag* RNA for dimerization and MA(p15)-binding activities, we applied a simple cDNA probing method on the basis of the following assumptions: that short single-stranded DNA probes complementary to the U5-5′ *gag* sequences can hybridize to the nascent RNA chains generated by the polymerase reaction, which results in masking of the active sequences and/or disruption of the inherent folding by imposition of an RNA/DNA double helix; and that subsequent electrophoretic analysis in combination with the protein binding reaction permits the estimation of the active regions. Two sets of cDNA probing assays were carried out as described in Materials and Methods. cDNA probes of 18 or 30 bases were synthesized to scan the RNA sequences as shown in Fig. 1. Probe 4.4 was directed to 30 bases in the 3′ part of the R region, which is not contained in the U5-5′ *gag* RNA and therefore used as an inactive cDNA probe.

In the first assay, each cDNA was ^{32}P phosphorylated at the 5′ terminus and added to the SP6 RNA polymerase reaction. Recovered RNA was electrophoresed through a nondenaturing gel to monitor dimerization and complex formation efficiency. Typical results are shown in Fig. 2A. The cold U5-5′ *gag* RNA probed with various ^{32}PcDNAs (odd-numbered lanes with the exception of lanes 1 and 9) appeared as dimer and monomer bands at the positions corresponding to those of the internally labeled U5-5′ *gag* RNA (lanes 1 and 9). Probe 4.4 failed to form a detectable band (lane 17). Unhybridized probe molecules made a broad band at the bottom of each lane.

As described previously, the U5-5′ *gag* RNA efficiently dimerized to form the dimer and monomer bands in a ratio of 4:1 on the basis of the radioactivity count in each band (lane 1). Hybridization of probes 1.1, 7.2, and 1.3 (lanes 21, 23, and 13) affected the RNA dimerization to alter the ratio of dimer/monomer populations to 1:4, 1:5, and 1:1, respectively. Other cDNAs did not appear to impair dimer formation, although their hybridization efficiencies were not significantly different from those of the three inhibitory probes, as compared by the band intensities.

After incubation with the MA(p15) protein, U5-5′ *gag* formed a shifted band presumed to contain the U5-5′ *gag* dimer (Fig. 2A, lanes 2 and 10). It is thought that MA(p15) has an RNA-annealing activity concomitant with the binding activity (17). By mild heat treatment of the RNA prior to the protein binding reaction, both the dimer and monomer shifts became detectable in the same lane, as described previously. On a 3.5% polyacrylamide gel, the two band shifts were detected by 30% reduction in their mobilities. In a parallel experiment on a 2.5% polyacrylamide–0.5% agarose composite gel, their shifts were found as 60 to 70% slower migration than for the free dimers and monomers. From these observations, shifted bands detected in this study were judged by their relative mobilities to represent either dimer or monomer complexes.

Many of the [^{32}P]cDNA/RNA hybrids normally reacted with the protein, as judged by the appearance of the shifted

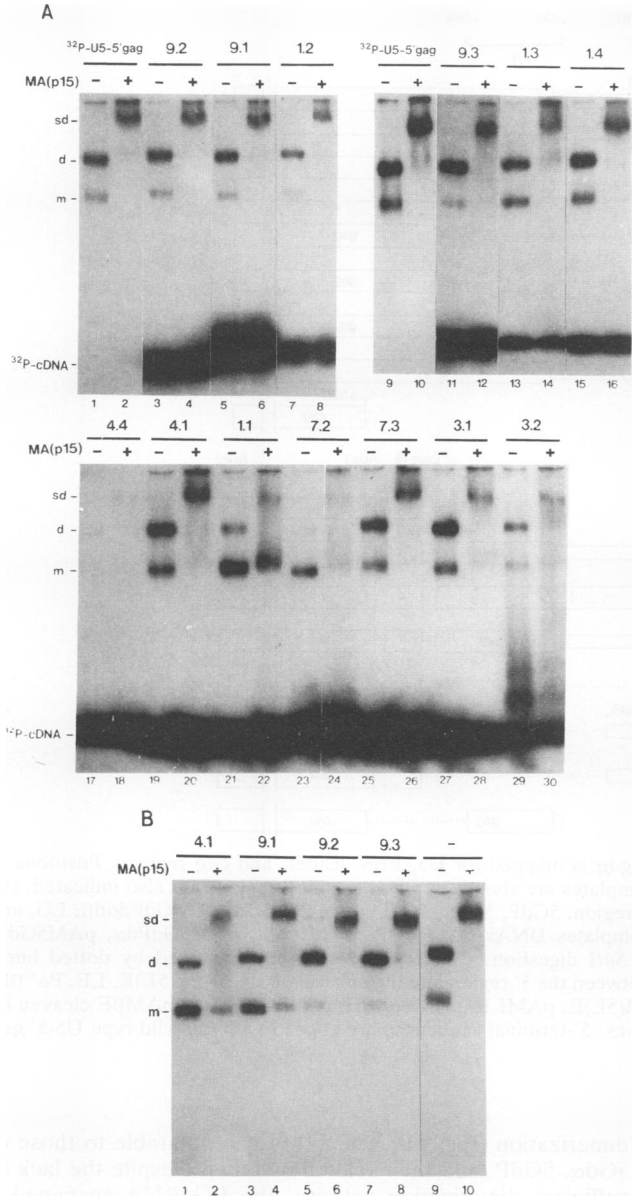

FIG. 2. Results of cDNA probing assays. (A) [^{32}P]cDNA probing assay. Unlabeled U5-5′ *gag* synthesized in the presence of ^{32}P-labeled cDNA was analyzed by polyacrylamide-agarose gel electrophoresis after incubation with (lanes +) or without (lanes −) MA(p15). Control experiments with ^{32}P-labeled U5-5′ *gag* are shown in lanes 1, 2, 9, and 10. Input cDNA is indicated for each set of experiments. Positions of dimers (d), monomers (m), and shifted dimers (sd) of U5-5′ *gag* RNA are indicated. The position of free [^{32}P]cDNA is also indicated. Lanes are numbered at the bottom. Binding of 9.3, 9.4, 3.3, and 3.4 did not interfere with either dimer formation or protein binding. (B) Probing assay with unlabeled cDNA. Results with probes 4.1, 9.1, 9.2, and 9.3 as well as results of a control experiment (−) are shown. Probes 4.1 and 9.1 impaired the dimer formation of ^{32}P-labeled U5-5′ *gag* and also affected band retardation. Results with probes 9.2, 9.3, and other cDNAs were similar to those shown in panel A.

dimer band (Fig. 2A, lanes 4, 6, 8, 12, 16, 20, and 26). In contrast, U5-5′ *gag* hybridized with probe 1.1 or 7.2 exhibited unusual electrophoretic features after incubation with MA(p15). As observed in lane 22, the dimers of the RNA/1.1 hybrid shifted normally, while the monomers stayed at the free position. The RNA/7.2 hybrids made no clear band shift and formed a diffusion through lane 24. Another notable profile was observed with probes 3.1 and 3.2 (lanes 27 to 30). Although dimers were formed in the same efficiency as in the control U5-5′ *gag* RNA, disruption of the shifted band was detected (lanes 28 and 30). An extended smear was formed along lane 30.

In the second cDNA probing assay, the RNA polymerase reaction contained [α-^{32}P]CTP as a labeled nucleoside triphosphate and unlabeled probe cDNA so that effects of the input probe were monitored by the radiolabel within the body of the RNA. Results obtained in this probing method were similar to those in the first experiments; however, probes 4.1 and 9.1 obviously inhibited dimerization (Fig. 2B, lanes 1 and 3). The dimerized RNA in the presence of probe 4.1 or 9.1 was observed to form complexes with MA(p15). The monomers were less reactive than the control monomers, and long smears were found between the shifted dimers and free monomers (lanes 2 and 4). Probes 4.1 and 9.1 had a complementary stretch within their sequences, which may have resulted in a different binding feature after a phosphorylation reaction containing spermidine.

From the results of the two cDNA probing experiments, dimer formation was suspected in the sequences covered with probes 9.1, 4.1, 1.1, and 7.2. Since probes 1.3 and 7.2 had 19 bases in common, the weak interfering activity of probe 1.3 was represented by probe 7.2. The MA(p15) binding was expected to involve the dimer-forming regions and the sequences covered with 3.1 and 3.2 (Fig. 1C and D). For convenience, the 7.2-, 3.1 + 3.2-, and 4.1 + 9.1-directed regions are referred to as α, β, and γ, respectively.

Deletion analysis of U5-5′ *gag*. To confirm that the α, β, γ, and PBS regions are related to dimer formation and complex formation, a deletion experiment was carried out. Structures of the mutant RNAs synthesized are illustrated in Fig. 3A. In the structure names, dP, dα, and dβ are used to represent specific deletions as follows: dP, deletion of the 3′-terminal 17 or 12 bases of U5 and the adjacent 18 bases of PBS; dα, deletion of the 25 bases of the α region; and dβ, deletion of the sequences from +373 to +487 harboring the β region. The wild-type and mutant RNAs were synthesized with ^{32}P label in parallel reactions and analyzed for their dimerization and MA(p15)-binding abilities.

Only 20% of the RNA molecules in the 5Gdα, 5GdP, and 5GdPdα preparations were dimerized (Fig. 4A), suggesting that removal of either the PBS or α region results in a loss of the dimerization potential of U5-5′ *gag*. These mutant monomers did not make a discrete band shift after the MA(p15) binding reaction (lanes 4, 6, and 8), while the dimers were able to make a clear shift as did the wild-type RNA (lane 2).

Deletion of the β-containing region did not alter the dimerization efficiency (lane 11). However, only 40% of the 5Gdβ dimer population participated in the complex formation with MA(p15) (lane 12). Moreover, the dimer complex did not appear as a firm band. These results indicate that the β region is not required for RNA dimerization but may be involved in the protein binding reaction.

5Gdαdβ and 5GdPdαdβ also poorly dimerized (Fig. 4A, lanes 13 and 15). Their dimer shifts (in lanes 14 and 16) were not solid as those of 5Gdα, 5GdP, and 5GdPdα. The control *gag* RNA made no band shift after the protein binding

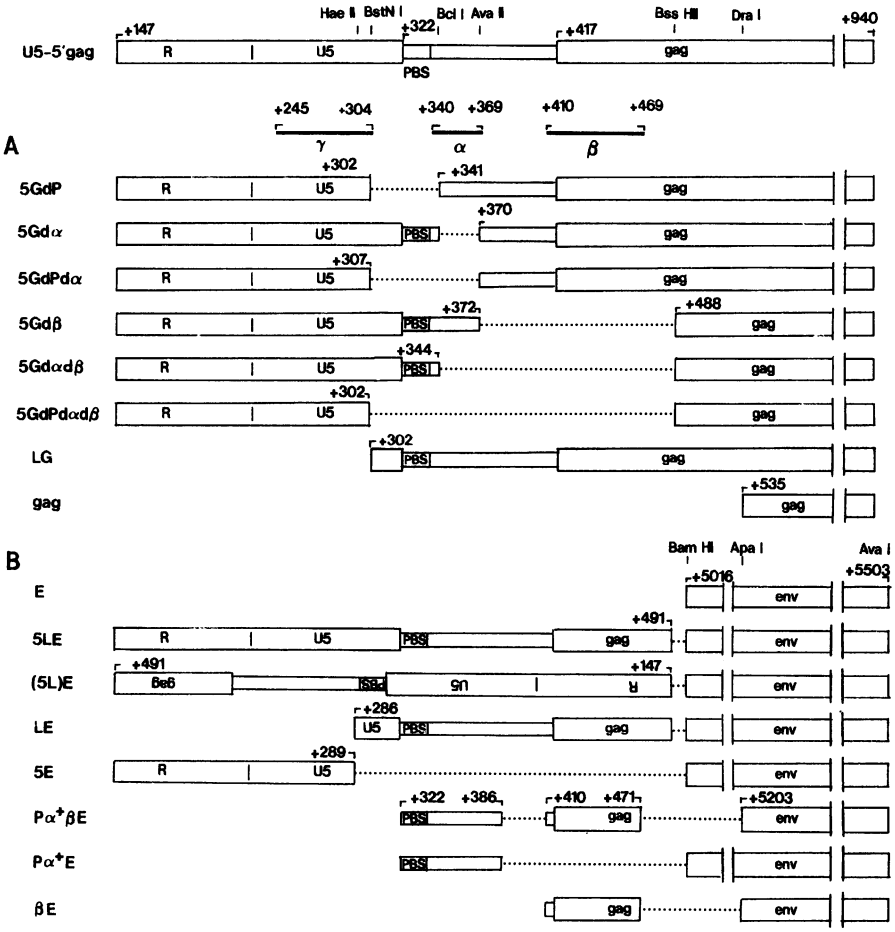

FIG. 3. Structures of deletion and fusion mutants. Wild-type U5-5′ *gag* is mapped for U5, PBS, leader, and *gag* regions. Positions of restriction enzyme cleavage sites used for the construction of mutant templates are shown. γ, PBS, α, and β regions are also indicated. (A) RNAs with various deletions in the leader and/or 5′ terminus of the *gag* region. 5GdP, 5Gdα, 5GdPdα, 5Gdβ, 5Gdαdβ, 5GdPdαdβ, LG, and *gag* were synthesized by SP6 RNA polymerase reactions using as templates DNAs pAM5GdP, pAM5Gdα, pAM5GdPdα, pAM5Gdβ, pAM5Gdαdβ, pAM5GdPdαdβ, pAMLG, and pAMgag, linearized by *SalI* digestion. Deleted sequences are indicated by dotted lines. Nucleotide positions are also indicated. (B) Recombinant RNAs made between the 5′ region and the *env* region. E, 5LE, (5L)E, LE, Pα+βE, Pα+E, and βE were synthesized from templates pAME, pAM5LE, pAM(5L)E, pAMLE, pAMPα+βE, pAMPα+E, and pAMβE cleaved by *AvaI*. Linkages generated by gene manipulation are shown by dotted lines. 5′-terminal sequences are aligned with the wild-type U5-5′ *gag* shown above.

reaction (lane 10), although the dimer and monomer bands appeared to be slightly smeared.

Thus, in agreement with the results obtained in the cDNA probing assays, the deletion analyses (Fig. 4A) suggested that the PBS and α regions contribute primarily to dimer formation and that β sequences contribute to MA(p15) binding.

To compare the affinities for MA(p15) among wild-type and mutant RNAs, we next performed competition assays with unlabeled U5-5′ *gag* RNA as described previously (Fig. 4B). In the wild-type RNA, 90 and 40% of the total radioactivities were retained in the shifted dimer band in the presence of 10- and 100-fold excess amounts of the cold competitor, respectively (lanes 3 and 4). In contrast, the complexes of 5GdPdα, 5Gdβ, and 5GdPdαdβ RNAs were effectively dissociated by a 10-fold concentration of the wild-type RNA. Less than 5% of the input ^{32}P counts were found in the retarded band in lanes 7, 10, and 13.

Another mutant, LG, consisting of the whole L region and the *gag* sequences, had an interesting phenotype. The rate of dimerization (Fig. 4B, lane 14) was comparable to those of 5Gdα, 5GdP, and their related mutants. Despite the lack of sufficient dimerization activity, the LG RNA sustained a more intense reactivity with MA(p15) than did 5Gdα, 5GdP, 5Gdβ, or the related mutants. The LG RNA made an additional band of slower migration representing the monomer complex as well as the band of shifted dimers (lane 15). In addition, one-fourth of the input monomer population was incorporated into the dimer complexes after incubation with MA(p15); the dimer complex in lanes 15 and 16 contained an increased ^{32}P radioactivity. Moreover, the LG dimer-MA(p15) complex was retained in the competition assay with 10-fold concentration of the wild-type RNA (lane 16) but not the monomer-MA(p15) complex. The γ region likely participates in the RNA dimerization but is less responsible for MA(p15) binding and the MA(p15)-induced RNA dimerization.

Experiments with recombinant RNAs. We tested whether the γ, PBS, α, and β sequences can exert their functions when linked 5′ to the *env* sequences that are not directly

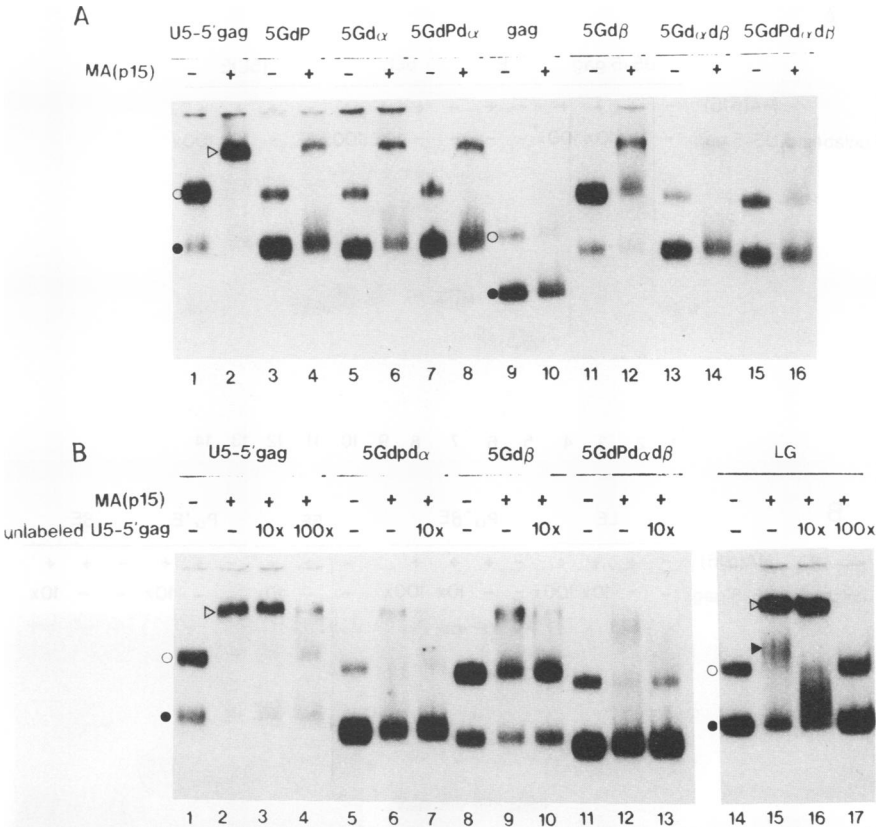

FIG. 4. Analysis of deletion mutants for dimer formation and complex formation with MA(p15). (A) MA(p15) binding assay with mutants having deletions in the PBS-leader region. The wild-type and mutant RNAs were incubated with (lanes +) or without (lanes −) MA(p15) (25 μM) and analyzed on a native gel. Positions of dimers and monomers are indicated by open and filled circles, respectively, for the U5-5′ *gag* and *gag* RNAs (lanes 1 and 9). The complex of the U5-5′ *gag* RNA dimer and MA(p15) is indicated by a triangle in lane 2. (B) Band shift and competition assays. U5-5′ *gag* and mutant RNAs with deletions in the PBS-leader or R-U5 region were examined for MA(p15)-binding ability. In the competition assays, concentrations of the wild-type competitor, U5-5′ *gag*, are indicated as 10× (10-fold) or 100× (100-fold) in comparison with that of the labeled RNA. −, reactions without the competitor.

related to the packaging mechanism. A series of recombinant RNAs synthesized for this purpose is shown in Fig. 3B, and the results of the MA(p15) binding assay are shown in Fig. 5. The control *env* RNA, E, was poorly dimerized, and it did not make a discrete band shift after the MA(p15) binding reaction (Fig. 5A, lanes 5 and 6).

The 5LE RNA with a sense insertion of the 5′-terminal portion of U5-5′ *gag* formed a solid dimer band containing 40% of the total ^{32}P radioactivity (Fig. 5A, lane 7) and made a clear dimer shift (lane 8) similar to that of U5-5′ *gag* (lanes 2 to 4). The monomer shift was not detectable as a firm band. The recombinant RNA retained the protein-binding activity in the competition assay with a 10-fold excess amount of the cold U5-5′ *gag* RNA (lane 9) but not with a 100-fold concentration of the competitor (lane 10). In contrast, (5L)E with the opposite strand of the U5-leader region was deficient in both self-dimerization and complex formation with MA(p15) (lanes 11 to 14). These results indicate that the positive strand of the U5-leader segment from positions +147 to +491 bears minimum structural requirements for the two RNA functions.

Neither the LE RNA containing the complete leader sequences nor 5E with the U5 region dimerized sufficiently (Fig. 5B, lanes 1 and 9) in comparison with 5LE (Fig. 5A, lane 7), ensuring the cooperation of U5 with PBS-leader region in viral RNA dimerization. LE could make the monomer and dimer band shifts firmly; shifts were, however, prevented by the 10-fold concentration of U5-5′ *gag* (Fig. 5B, lanes 1 to 4). The Pα$^+$βE RNA with PBS-α and β elements in a truncated form made a band shift profile similar to that of LE (lanes 5 to 8) but less efficiently.

Dimers of 5E behaved like those of 5GdPdαdβ (Fig. 4B, lanes 11 to 13) after the protein binding reaction (Fig. 5B, lanes 9 to 11), while monomers smeared through lane 10. Neither Pα$^+$E nor βE formed a visible dimer band. The Pα$^+$E monomers failed to give a clear shift in lane 13, while the βE monomers could form a broad and diffuse band barely separated from the unbound monomer band (lane 16) in the absence of the wild-type competitor. The results in Fig. 5B indicate that each of the small elements in the U5-PBS-α-β region is poorly reactive to MA(p15).

It should be noted that the *gag*-tailed RNAs, 5G and LG, were significantly more active in dimerization as well as in complex formation than were the corresponding *env*-tailed RNAs, 5LE and LE, respectively. Since the *gag* region from position +535 to +940 itself had a detectable dimer-forming nature but did not cause the band shift with MA(p15) (Fig. 4A, lanes 9 and 10), it is likely that the *gag* RNA structure influences the overall RNA folding and thereby supports the upstream RNA functions.

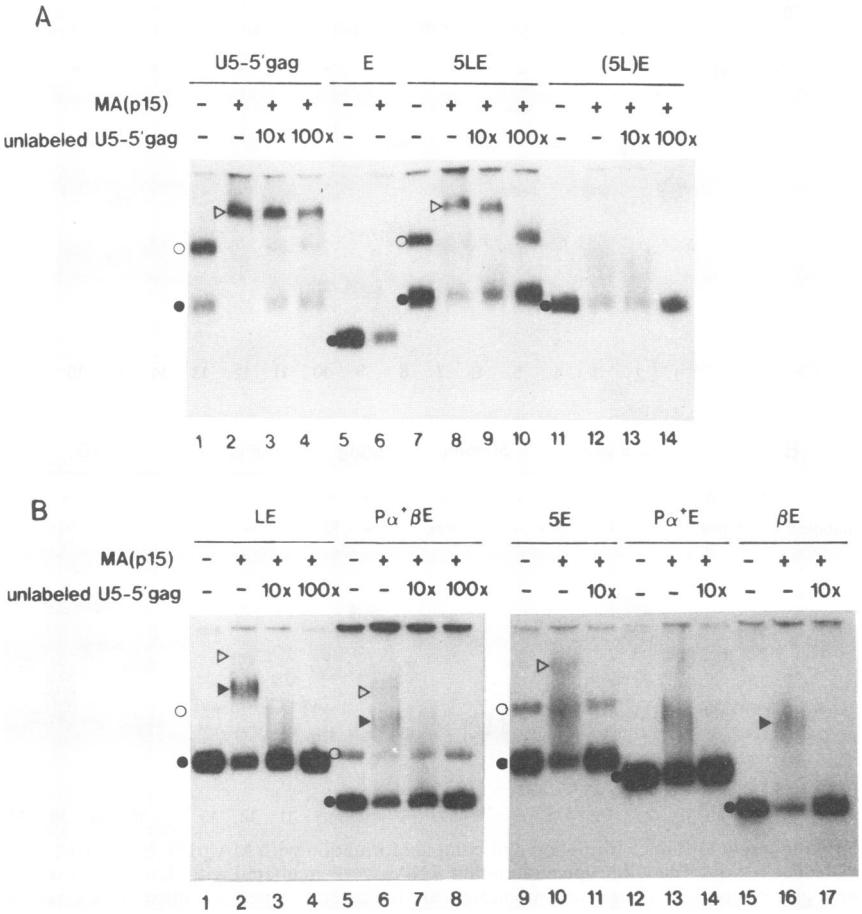

FIG. 5. Analysis of recombinant RNAs for dimerization and MA(p15)-binding activities. (A) Results for the parental RNAs, U5-5′ *gag*, and E and for recombinant RNAs, 5LE, and (5L)E; (B) results for other recombinants containing short segments from the 5′-terminal region and the body of the *env* region. The monomer band of each RNA is indicated by a filled circle. Detectable dimer bands are marked with open circles. Shifted dimers and monomers are shown by triangles and filled triangles, respectively. Samples were incubated with MA(p15) (+) or in buffer alone (−). Concentrations of the competitor U5-5′ *gag* are indicated as 10× (10-fold) or 100× (100-fold) relative to the test RNA concentration.

Computer-assisted analysis of BLV 5′-terminal RNA folding. The dimer-forming and MA(p15)-binding sequences determined above were examined for their formation of secondary structures by free-energy minimization analysis.

As shown in Fig. 6A, a branched stem-loop structure was predicted in the region encompassing U5 to the α region. In the prediction, the U5 sequences form long stems II and IV, a short stem III, and associated bulges and loops. The PBS and α sequences form stem V. Three base pairings between the 5′ terminus of U5 and the 3′ terminus of α make stem I.

In the β region, two separate stem-loop structures VI and VII, consisting of residues +417 to +437 and +447 to +471, respectively, were predicted (Fig. 6B). Stem-loop VI is complementary to cDNA probe 3.1 and stem-loop VII is complementary to probe 3.2, which may account for their inhibitory effect on the MA(p15) binding reaction (Fig. 2A).

DISCUSSION

Dimerization of BLV and other retrovirus RNA. We have examined the dimer-forming feature of the 5′-terminal BLV RNA by a cDNA probing method and mutation experiments with the U5-5′ *gag* RNA fragments. All of the experimental results may be interpreted as implying that RNA dimerization is mediated by the region encompassing U5, PBS, and the 3′ flanking 30 bases of PBS (α).

Computer-assisted RNA sequence analysis suggested formation of a secondary structure of a stem-loop with multiple branches throughout the entire region determined. In that model, the γ sequences contribute to stem-loops II, III, and IV. Eleven residues of PBS and one base of its 5′ adjacent region are found to pair with the α sequences to make stem V. Because retrovirus RNA dimerization is assumed to result from intermolecular base pairings due to the presence of palindromic sequences (8), the model seems to support our data.

Stem-loop V is analogous to the secondary structure proposed for avian retrovirus RNAs, in which the 3′ U5-PBS region hybridizes the 5′-terminal leader sequences to build up a more extended stem without branching (2, 13). The involvement of the PBS-α region in BLV RNA dimerization agrees with the dimer model predicted for avian and murine viruses in earlier studies (8).

We have also analyzed HIV RNA for dimer formation by cDNA probing. The preliminary result shows that the 5′-terminal extended stem-loop II of the reported secondary

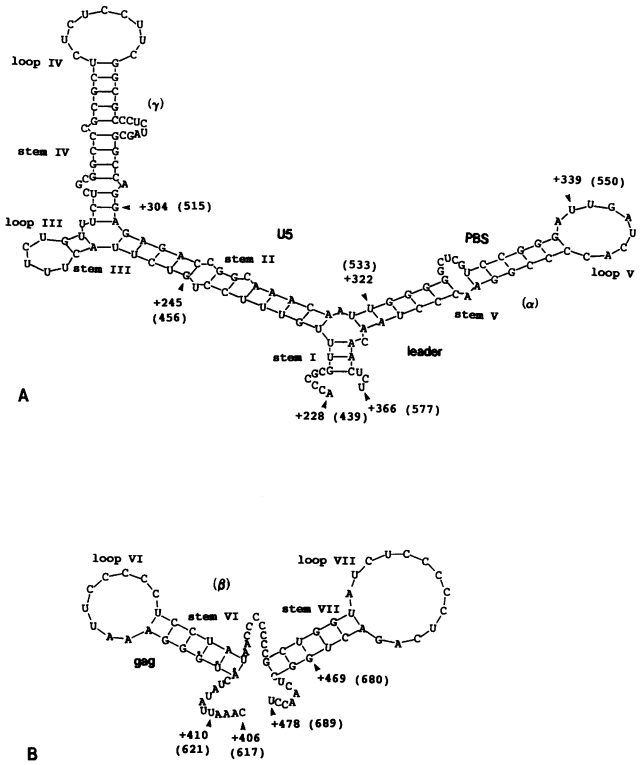

FIG. 6. RNA secondary structures predicted for the dimer-forming and MA(p15)-binding regions by computer-assisted energy minimization analysis. (A) Multibranched stem-loop structure formed by the dimerization sequences +228 to +366. Nucleotide numbers originate from the RNA cap site (+1). Position numbers in the sequenced provirus genome (38) are also shown in parentheses. Stems I to IV and associating loops are indicated. The start (+245) and end (+304) positions of the γ region and of PBS (+322 and +339) are marked. Nucleotide numberings in the proviral genome are also indicated in parentheses. (B) Two stem-loops found in the β region. Sequences from +406 to +478 were analyzed for secondary structure. The AUG translation start codon of the *gag* gene is marked by dots. The β region encompassed nucleotides +410 to +469. Stem-loops VI and VII are indicated.

structure in the HIV leader (12) is probably involved in dimerization and that U5 and PBS may not be required.

The MuLV dimerization site has been reported to be present within the ψ sequences, where a double stem-loop was predicted (37). However, the folding of the recent prediction deviates from the long-standing model (8) and seems to be comparable to the BLV β structure with regard to both location and overall structure.

BLV RNA dimerization and primer tRNA^{Pro} binding. In retrovirus particles, tRNA primer binding is compatible with genome RNA dimerization (8). A primer-associated RNA dimer model, as well as a primer-free dimer model, was proposed for avian and mouse retroviruses (8, 13). However, it is inferred from our cDNA probing and deletion analyses that BLV RNA dimerization is competitive with tRNA^{Pro} binding; binding of cDNA 1.1 and deletion of PBS inhibited the dimerization. Also, it should be noted that the 3'-terminal primer tRNA sequences are locked in the characteristic cloverleaf structure by formation of the acceptor and TψC stems. The process of tRNA annealing may be a more sophisticated dynamic reaction than has been interpreted by earlier experiments (35). Unfolding of the genome RNA dimer structure, in addition to unwinding of the tRNA stems (11), might be involved.

RNA structures required for MA(p15) binding. Deletion and chimeric mutation analyses implicate the region encompassing PBS to the 5' end of the *gag* sequences, PBS-α-β, as sequences essential for the specific interaction with MA(p15) to make a complex that is detected as a discrete band in the gel retardation assay. The β region was predicted to form two isolated stem-loops VI and VII, while the PBS-α region likely forms stem-loop V, involved in the dimer conformation as described above.

It is possible that PBS-α and β cooperatively make a three-dimensional conformation active in protein binding. It is also possible that the PBS-α region in concert with the *gag* sequences exhibits the dimer-forming activity and thereby increases the affinity of the β structure to the protein.

BLV U5-5' *gag*-MA(p15) complex formation and genome packaging. Although there has been no direct information about BLV genome RNA packaging, our in vitro characterization of U5-5' *gag*-MA(p15) complex formation is related to the accumulated experimental results concerning the genome encapsidation in MuLV and other retrovirus systems from the viewpoints described below.

PBS-α-β covers the BLV RNA region analogous to the packaging sites determined for MuLV (28, 41), Rous sarcoma virus (33), avian sarcoma-leukosis virus (18, 43), spleen necrosis virus (45), and HIV (3, 23). Recent observation that *gag* sequences are also included in the signal sufficient for heterologous RNA packaging into MuLV and Rous sarcoma virus virions (1, 5–7) supports our results; the BLV β region contained the *gag* start codon and its 3' sequences. In addition, the downstream *gag* sequences were found to perform facilitating roles in the MA(p15) binding reaction.

Further support is provided by the fact that deletions in the U5 region of the MuLV genome resulted in blocking of the RNA packaging into the virus particles (32). In this study with BLV RNA, U5 was shown to contain a part of the region essential for RNA dimerization. Deletion of U5 resulted in a more than a 10-fold decrease in complex-forming ability (compare LG with U5-5' *gag* in Fig. 4B), although the RNA feature to be annealed upon MA(p15) binding was retained. These notions agree with the explanation that the U5 region of MuLV may not be directly involved in the selective packaging of viral RNA but is required to maintain the correct overall structure of the viral genome (24).

BLV RNA dimerization appeared to lead to enhanced reactivity with MA(p15) protein. Conversely, MA(p15) binding often resulted in annealing of the RNA monomers. These observations could offer an explanation for why retrovirus particles contain a 70S dimer as the genome.

With all of these in vitro results, it is necessary to determine at the cell culture level the RNA and protein sequences required for BLV packaging, using a DNA clone capable of infectious particle production or an equivalent assay system.

There is disagreement concerning the function of avian retrovirus MA(p19); the specific RNA-binding activity described in earlier studies (20, 21) was undetectable in recent experiments (42). Furthermore, detection of the specific interaction between MuLV pp12 and the homologous RNA (39, 40) has never been repeated with other methods or further investigated to determine the responsive RNA sequences. Since retrovirus *gag* precursor processing occurs

after formation of the immature core (19, 47), it is the *gag* polyprotein that first associates with the viral RNA. Unlike avian virus MA(p19) or MuLV pp12, BLV MA(p15) is the NH_2-terminal cleavage intermediate generated by the $Pr44^{gag}$ processing (46) or the precursor of mature proteins MA(p10) and p4 (17).

The 5′-terminal RNA structure and virus replication. In the predicted folding of the β region (Fig. 6B), the *gag* start codon is found in stem VI. Although the model needs to be validated experimentally, it is conceivable that the 5′-terminal conformation of the viral RNA and its interaction with cellular and viral proteins may determine the fate of viral RNA molecules either to act as mRNA or to be encapsidated into particles as the genome RNA. In HIV, the large folded structure lies immediately 5′ to the AUG codon (12).

Many functional elements for reverse transcription priming, RNA dimerization, packaging, translation initiation and activation, and splicing nest in the 5′-terminal region of retroviral RNA. Some of these elements overlap each other or are in close proximity, suggesting the possibility that one RNA function can regulate other activities. The 5′-terminal region may form an intricate three-dimensional conformation. In this regard, retroviral RNA may be reminiscent of poliovirus RNA, whose 5′-terminal noncoding region forms a defined cloverleaf structure that controls translation (34, 44) and genome replication (4) by interacting with various cellular and viral factors.

ACKNOWLEDGMENT

We thank Yoko Sakamoto for BLV preparation.

REFERENCES

1. **Adam, M. A., and A. D. Miller.** 1988. Identification of a signal in a murine retrovirus that is sufficient for packaging of nonretroviral RNA into virions. J. Virol. **62**:3802–3806.
2. **Aiyar, A., D. Cobrinik, S. Ge, H.-J. Kung, and J. Leis.** 1992. Interaction between retroviral U5 RNA and the TψC loop of the $tRNA^{Trp}$ primer is required for efficient initiation of reverse transcription. J. Virol. **66**:2464–2472.
3. **Aldovini, A., and R. A. Young.** 1990. Mutations of RNA and protein sequences involved in human immunodeficiency virus type 1 packaging result in production of noninfectious virus. J. Virol. **64**:1920–1926.
4. **Andino, R., E. Rieckhof, and D. Baltimore.** 1990. A functional ribonucleoprotein complex forms around the 5′ end of poliovirus RNA. Cell **63**:369–380.
5. **Armentano, D., S.-F. Yu, P. W. Kantoff, T. von Ruden, W. F. Anderson, and E. Gioboa.** 1987. Effect of internal viral sequences in the utility of retroviral vectors. J. Virol. **61**:1639–1646.
6. **Aronoff, R., and M. Linial.** 1991. Specificity of retroviral RNA packaging. J. Virol. **65**:71–80.
7. **Bender, M. A., T. D. Palmer, R. E. Glinas, and A. D. Miller.** 1987. Evidence that the packaging signal of Moloney murine leukemia virus extends into the *gag* region. J. Virol. **61**:1639–1646.
8. **Coffin, J.** 1982. Structure of the retroviral genome, p. 261–368. *In* R. Weiss, N. Teich, H. Varmus, and J. Coffin (ed.), RNA tumor viruses. Cold Spring Harbor Laboratory, Cold Spring Harbor, N.Y.
9. **Gorelick, R. J., L. E. Henderson, J. P. Hanser, and A. Rein.** 1988. Point mutants of Moloney murine leukemia virus that fail to package viral RNA: evidence for specific RNA recognition by a "zinc finger-like" protein sequence. Proc. Natl. Acad. Sci. USA **85**:8420–8424.
10. **Gorelick, R. J., S. M. Nigida, Jr., J. W. Bess, Jr., L. O. Arthur, L. E. Henderson, and A. Rein.** 1990. Noninfectious human immunodeficiency virus type 1 mutants deficient in genomic RNA. J. Virol. **64**:3207–3211.
11. **Harada, F., G. G. Peters, and J. E. Dahlberg.** 1979. The primer tRNA for Moloney murine leukemia virus DNA synthesis. J. Biol. Chem. **254**:10979–10985.
12. **Harrison, G. P., and A. M. L. Lever.** 1992. The human immunodeficiency virus type 1 packaging signal and major splice donor region have a conserved stable secondary structure. J. Virol. **66**:4144–4153.
13. **Haseltine, W. A., A. M. Maxam, and W. Gilbert.** 1977. Rous sarcoma virus genome is terminally redundant: the 5′ sequence. Proc. Natl. Acad. Sci. USA **74**:989–993.
14. **Heaphy, S., C. Dingwall, I. Ernberg, M. J. Gait, S. M. Green, J. Karn, A. D. Lowe, M. Singh, and M. A. Skinner.** 1990. HIV-1 regulator of virion expression (Rev) protein binds to an RNA stem-loop structure located within the Rev response element region. Cell **60**:685–693.
15. **Jentoft, J. E., L. M. Smith, X. Fu, M. Johnson, and J. Leis.** 1988. Conserved cysteine and histidine residues of the avian myeloblastosis virus nucleocapsid protein are essential for viral replication but are not "zinc-binding fingers." Proc. Natl. Acad. Sci. USA **85**:7094–7098.
16. **Karpel, R. L., L. E. Henderson, and S. Oroszlan.** 1987. Interactions of retroviral structural proteins with single-stranded nucleic acids. J. Biol. Chem. **262**:4961–4967.
17. **Katoh, I., H. Kyushiki, Y. Sakamoto, Y. Ikawa, and Y. Yoshinaka.** 1991. Bovine leukemia virus matrix-associated protein MA(p15): further processing and formation of a specific complex with the dimer of the 5′ terminal genomic RNA fragment. J. Virol. **65**:6845–6855.
18. **Katz, R. A., R. W. Terry, and A. M. Skalka.** 1986. A conserved *cis*-acting sequence in the 5′ leader of avian sarcoma virus RNA is required for packaging. J. Virol. **59**:163–167.
19. **Kohl, N. E., E. A. Emini, W. A. Schleif, L. J. Davis, J. C. Heimbach, R. A. F. Dixon, E. M. Scolnick, and I. S. Sigal.** 1988. Active human immunodeficiency virus protease is required for viral infectivity. Proc. Natl. Acad. Sci. USA **85**:4686–4690.
20. **Leis, J., S. Johnson, L. S. Collins, and J. A. Traugh.** 1984. Effects of phosphorylation of avian retrovirus nucleocapsid protein pp12 on binding of viral RNA. J. Biol. Chem. **59**:7726–7732.
21. **Leis, J., J. McGinnis, and R. W. Green.** 1978. Rous sarcoma virus p19 binds to specific double-stranded regions of viral RNA: effect of p19 on cleavage of viral RNA by RNase III. Virology **84**:87–98.
22. **Lenardo, M. J., C.-M. Fan, T. Maniatis, and D. Baltimore.** 1989. The involvement of NF-κB in β-interferon gene regulation reveals its role as widely inducible mediator of signal transduction. Cell **57**:287–294.
23. **Lever, A., H. Gottlinger, W. Haseltine, and J. Sodroski.** 1989. Identification of a sequence required for efficient packaging of human immunodeficiency virus type 1 RNA into virions. J. Virol. **63**:4085–4087.
24. **Linial, M. L., and A. D. Miller.** 1990. Retroviral RNA packaging: sequence requirements and implications. Curr. Top. Microbiol. Immunol. **157**:125–152.
25. **Lowry, O. H., N. J. Rosebrough, A. L. Farr, and R. J. Randall.** 1951. Protein measurement with the Folin phenol reagent. J. Biol. Chem. **193**:265–275.
26. **Luban, J., and S. P. Goff.** 1991. Binding of human immunodeficiency virus type 1 (HIV-1) RNA to recombinant HIV-1 *gag* protein. J. Virol. **65**:3203–3212.
27. **Malim, M. H., L. S. Tiley, D. F. McCarn, J. R. Rusche, J. Hauber, and B. R. Cullen.** 1990. HIV-1 structural gene expression requires binding of the Rev trans-activator to its RNA target sequence. Cell **60**:675–683.
28. **Mann, R., R. C. Mulligan, and D. Baltimore.** 1983. Construction of a retrovirus packaging mutant and its use to produce helper-free defective retrovirus. Cell **33**:153–159.
29. **Meric, C., and S. P. Goff.** 1989. Characterization of Moloney murine leukemia virus mutants with single-amino-acid substitutions in the Cys-His box of the nucleocapsid protein. J. Virol. **63**:1558–1568.
30. **Meric, C., E. Gouilloud, and P.-F. Spahr.** 1988. Mutations in Rous sarcoma virus nucleocapsid protein p12 (NC): deletions of

Cys-His boxes. J. Virol. **62**:3328–3333.
31. **Meric, C., and P.-F. Spahr.** 1986. Rous sarcoma virus nucleic acid-binding protein p12 is necessary for viral 70S RNA dimer formation and packaging. J. Virol. **60**:450–459.
32. **Murphy, J. E., and S. P. Goff.** 1989. Construction and analysis of deletion mutations in the U5 region of Moloney murine leukemia virus: effects on RNA packaging and reverse transcription. J. Virol. **63**:319–327.
33. **Nishizawa, M., T. Koyama, and S. Kawai.** 1985. Unusual feature of the leader sequence of Rous sarcoma virus packaging mutant TK15. J. Virol. **55**:881–885.
34. **Pelletier, J., and N. Sonenberg.** 1988. Internal initiation of translation of eukaryotic mRNA directed by a sequence derived from poliovirus RNA. Nature (London) **334**:320–325.
35. **Peters, G., and J. E. Dahlberg.** 1979. RNA-directed DNA synthesis in Moloney murine leukemia virus: interaction between the primer tRNA and the genome RNA. J. Virol. **31**:398–407.
36. **Phalguni, G., and J. F. Ferrer.** 1980. Detection of a precursor-like protein of bovine leukemia virus structural polypeptides in purified virions. J. Gen. Virol. **47**:311–322.
37. **Prats, A. C., C. Roy, P. Wang, M. Erard, V. Housset, C. Gabus, C. Paoletti, and J.-L. Darlix.** 1990. *cis* elements and *trans*-acting factors involved in dimer formation of murine leukemia virus RNA. J. Virol. **64**:774–783.
38. **Sagata, N., T. Yasunaga, J. Tsuzuku-Kawamura, K. Ohishi, Y. Ogawa, and Y. Ikawa.** 1985. The nucleotide sequence of the genome of bovine leukemia virus: its evolutionary relationship to other retroviruses. Proc. Natl. Acad. Sci. USA **82**:677–681.
39. **Sen, A., and G. J. Todaro.** 1976. Specificity of *in vitro* binding of primate type C viral RNA and the homologous viral p12 core protein. Science **193**:326–328.
40. **Sen, A., and G. J. Todaro.** 1977. The genome-associated, specific RNA binding proteins of avian and mammalian type C viruses. Cell **10**:91–99.
41. **Sorge, J. D., D. Wright, V. D. Erdman, and A. E. Cutting.** 1984. Amphotropic retrovirus vector system for human cell gene transfer. Mol. Cell. Biol. **4**:1730–1737.
42. **Steeg, C. M., and V. M. Vogt.** 1990. RNA-binding properties of the matrix protein ($p19^{gag}$) of avian sarcoma and leukemia viruses. J. Virol. **64**:874–855.
43. **Stoker, A. W., and M. J. Bissell.** 1979. Development of avian sarcoma and leukosis virus-based vector-packaging cell lines. J. Virol. **62**:1008–1015.
44. **Trono, D., R. Andino, and D. Baltimore.** 1988. An RNA sequence of hundreds of nucleotides at the 5′ end of poliovirus RNA is involved in allowing viral protein synthesis. J. Virol. **62**:2291–2299.
45. **Watanabe, S., and H. M. Temin.** 1983. Encapsidation sequences for spleen necrosis virus, an avian retrovirus, are between the 5′ long terminal repeat and the start of the *gag* gene. Proc. Natl. Acad. Sci. USA **79**:5986–5990.
46. **Yoshinaka, Y., I. Katoh, T. D. Copeland, G. W. Smythers, and S. Oroszlan.** 1986. Bovine leukemia virus protease: purification, chemical analysis, and in vitro processing of *gag* precursor polyproteins. J. Virol. **57**:826–832.
47. **Yoshinaka, Y., and R. B. Luftig.** 1977. Murine leukemia virus morphogenesis: cleavage of P70 in vitro can be accompanied by a shift from a concentrically coiled internal strand ("immature") to a collapsed ("mature") form of the virus core. Proc. Natl. Acad. Sci. USA **74**:3446–3450.